

# Gadolinium Complex of $^{125}\text{I}/^{127}\text{I}$ -RGD-DOTA Conjugate as a Tumor-Targeting SPECT/MR Bimodal Imaging Probe

Ji-Ae Park,<sup>†</sup> Jung Young Kim,<sup>†</sup> Yong Jin Lee,<sup>†</sup> Wonho Lee,<sup>†</sup> Sang Moo Lim,<sup>‡</sup> Tae-Jeong Kim,<sup>§</sup> Jeongsoo Yoo,<sup>||</sup> Yongmin Chang,<sup>\*,||</sup> and Kyeong Min Kim<sup>\*,†</sup>

<sup>†</sup>Molecular Imaging Research Center and <sup>‡</sup>Department of Nuclear Medicine, Korea Institute of Radiological and Medical Sciences, Seoul 139-706, Republic of Korea

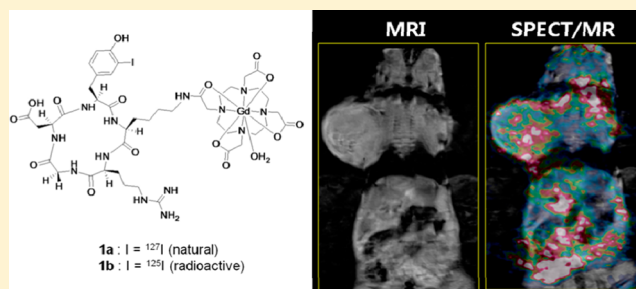
<sup>§</sup>Department of Applied Chemistry, Kyungpook National University, Daegu 702-701, Republic of Korea

<sup>||</sup>Department of Molecular Medicine, Kyungpook National University, Daegu 700-422, Republic of Korea

## S Supporting Information

**ABSTRACT:** The work describes the synthesis and in vivo application of  $[\text{Gd}(\text{L})(\text{H}_2\text{O})] \cdot x\text{H}_2\text{O}$ , where L is a ( $^{125}\text{I}/^{127}\text{I}$ -RGD)-DOTA conjugate, as a tumor-targeting SPECT/MR bimodal imaging probe. Here, ( $^{125}\text{I}/^{127}\text{I}$ -RGD)-DOTA signifies a “cocktail mixture” of radioisotopic (**1a**, L =  $^{125}\text{I}$ -RGD-DOTA) and natural (**1b**, L =  $^{127}\text{I}$ -RGD-DOTA) Gd complexes. The two complexes are chemically equivalent as revealed by HPLC, and their cocktail mixture exhibits the integrin-specific tumor enhancement, demonstrating that they constitute essentially a single bimodal imaging probe. Employment of a cocktail mixture thus proves to be a sole and practical approach to overcome the sensitivity difference problem between MRI and SPECT.

**KEYWORDS:** dual modality, SPECT/MR, RGD peptide, small molecule, tumor targeting



A accomplishment of multimodality molecular imaging is one of the ultimate goals in preclinical and clinical medicine. The combination of radioimaging and magnetic resonance imaging (MRI), among others, is the most plausible to visualize the molecular events in vivo because the combination can provide simultaneously high sensitivity and high resolution, which are prerequisites for effective molecular imaging.<sup>1,2</sup> Furthermore, contrary to optical imaging, neither radioimaging nor MRI does not suffer from the penetration depth problem, thus making it feasible to image deep organs. Single photon emission-computed tomography (SPECT) has widely been used in clinical radioimaging. SPECT, although it provides lower sensitivity and resolution than PET, possesses a unique advantage of clinical availability of many SPECT radioisotopes such as  $^{99\text{m}}\text{Tc}$ ,  $^{123}\text{I}$ ,  $^{201}\text{Tl}$ , and  $^{111}\text{In}$ . Besides, it is economic and convenient to use them in clinics as compared with PET isotopes.<sup>3,4</sup> In this work, we have used  $^{125}\text{I}$  as a source of  $^{123}\text{I}$  since  $^{125}\text{I}$  ( $T_{1/2} = 59.4$  days, 35 KeV) can readily turn into  $^{123}\text{I}$  ( $T_{1/2} = 13.2$  h, 159 KeV) for better SPECT imaging.

For the development of bimodal SPECT/MRI probes, one of the most important issues is how to overcome the sensitivity difference between SPECT and MRI, not to mention their chemical and structural differences. In general, the imaging sensitivity of SPECT is 6 orders of magnitude higher than that of MRI.<sup>4</sup> Thus, for example, the use of a 1:1 stoichiometry between SPECT and MRI probes leads the amount of the SPECT radioisotope far out of the safety limit for clinical usage.

Several methods have been proposed to overcome such difficulties.<sup>5,6</sup> One such attempt would involve incorporation of gadolinium dendrimers or nanomaterials with heavy loading capability of MRI agent.<sup>7</sup> Yet, even the nanobased MRI platform exhibits a sensitivity difference greater than 3 orders of magnitude. In addition, a serious drawback in the use of such nanoplatfroms lies in the fact that they exhibit a limited in vivo biodistribution. Namely, one study shows that less than 5% of a dual modal nanoplatfrom reaches the target site after intravenous injection, while the rest is taken up by reticuloendothelial system (RES).<sup>8</sup> Further practical limitations of nanoplatfroms may come from their inherent in vivo toxicity.<sup>9,10</sup>

An alternative approach for the design of a dual modality imaging agent is to use a low molecular weight bifunctional chelating agent (BFCA).<sup>11</sup> An advantage of Gd-BFCA as compared to gadolinium nanoparticles is that the former exhibits good in vivo biodistribution and as a result high target specificity without a significant RES uptake. For example, Dirksen has recently reported the synthesis of a gadolinium complex of DTPA-RGD conjugate incorporating a fluorescent dye for use as a tumor-specific MRI/optical dual modal imaging probe.<sup>12</sup> A major drawback of this probe is, as expected, the

Received: October 15, 2012

Accepted: December 17, 2012

Published: December 17, 2012

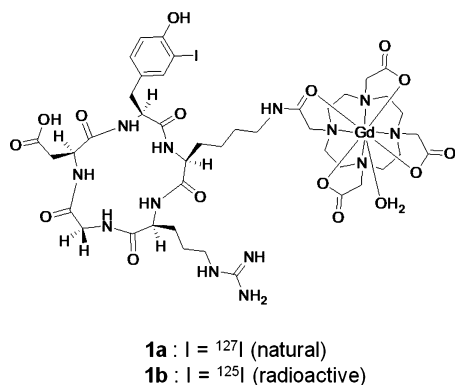
huge sensitivity difference between MR and optical images as a result of 1:1 stoichiometry of Gd-DTPA and the fluorescent dye within the same molecule.

We have recently demonstrated that the use of a “cocktail mixture” of two different probes would be an only alternative to overcome such a sensitivity difference and at the same time preserve the same in vivo biodistribution.<sup>13</sup> The BFCA is a binucleating DTPA-bis(histidylamide), and the cocktail mixture consists of Gd{DTPA-bis(histidylamide)} labeled with rhenium (Re)/technetium-99m (<sup>99m</sup>Tc). We have shown that both complexes are chemically equivalent and exhibit the same ex/in vivo biodistribution.<sup>13</sup> In this proof-of-concept study, radioactive <sup>99m</sup>Tc was substituted by Re in Gd{DTPA-bis(histidylamide)} to minimize the sensitivity difference between SPECT and MRI. One minor problem inherent to this cocktail mixture of Re/<sup>99m</sup>Tc has yet to be recognized, since the two isotopes are not identical (although similar). It would be therefore beneficial to use the same isotopes in a cocktail mixture.

For example, two iodine isotopes such as radioactive <sup>125</sup>I and nonradioactive <sup>127</sup>I form an identical pair and thus meet the requirement for the cocktail mixture. In our continued effort to develop a more sophisticated bimodal MR/SPECT imaging probe with a tumor-targeting nature, we have prepared a BFCA comprising DOTA and cyclic RGD (Arg-Gly-Asp), where cRGD is derivatized by <sup>125</sup>I/<sup>127</sup>I. cRGD is well-known to possess high and specific affinity for  $\alpha_v\beta_3$ -integrin and has been widely used as a molecular marker for tumor.<sup>14</sup> Yet, few studies are available on the synthesis and the application of <sup>125</sup>I/<sup>127</sup>I-RGD-DOTA as a BFCA.

<sup>127</sup>I-RGD, <sup>127</sup>I-RGD-DOTA, and the corresponding gadolinium complex (**1a**) were obtained in high yields (>95%) after HPLC purification. Their formation was confirmed by MALDI, and the purity of each compound was confirmed by the appearance of a single peak in the reverse-phase HPLC. Chart 1

Chart 1. Structure of Complexes 1



shows the structures of **1a,b**. Corresponding radioactive **1b** was obtained with a moderate radiochemical yield ( $\geq 40\%$ ) and purified by HPLC. Although radiochemical purity reaches as high as 99%, its use in in vivo assays and imaging is inappropriate due to the presence of acetonitrile (5%), an inner HPLC eluent. Thus, further purification can be achieved by purging a solution of **1b** with N<sub>2</sub> after which the specific activity of solid **1b** reaches up to 2200 Ci/mmol after drying. A solution of **1b** solution sterilized by a sterile filter (0.22  $\mu\text{m}$ ) was used for in vitro and in vivo studies.

The chemical equivalence of **1a** and **1b** can be established by analytical HPLC chromatography as demonstrated in Figure 1.

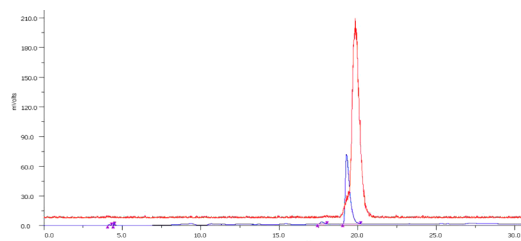


Figure 1. Analytical HPLC chromatograms of **1a** (blue, 254 nm) and corresponding **1b** (red,  $\gamma$  trace).

The figure shows the same retention times ( $R_t$ ) of 19.5 and 20.0 min for **1a** and **1b**, respectively. A slight difference in the retention times may be rationalized by different serial arrangement of the detectors with radiometric and UV detector.<sup>15</sup>

Both **1a** and **1b** reveal high stability in mouse serum for 3 days at 37 °C, demonstrating kinetic inertness toward degradation by endogenous enzymes. Figure 2a shows the in

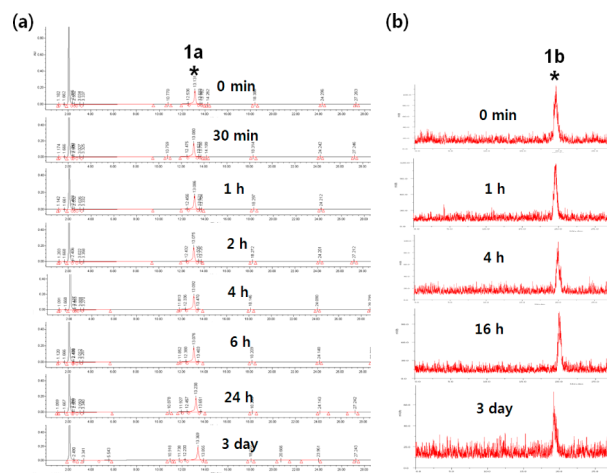


Figure 2. In vitro serum stability of **1a** (a) by UV detector at 254 nm and **1b** (b) by  $\gamma$  detector. The compounds were incubated in human serum at 37 °C and analyzed by HPLC at different time intervals.

vitro serum stability of **1a** as a function of time as measured by UV absorption. HPLC chromatograms show dissociations of RGD ( $R_t$ , 8.2 min), I-RGD ( $R_t$ , 12.8 min), I-RGD-DOTA ( $R_t$ , 12.6 min), and/or **1a**. Assignment of **1a** eluted at 13.1 min was made by comparison with a standard. The radiochromatographic profiles for serum samples with **1b** at different incubation times are shown in Figure 2b. The figure shows a single major peak ( $R_t$ , 20 min) assignable to **1b** regardless of the incubation time. No peak corresponding to free <sup>125</sup>I ( $R_t$ , 5 min) separated from **1b** was observed in 72 h of incubation.

The cytotoxicity of **1a** remains very low when incubated for 5 days (Figure S1 in the Supporting Information) and comparable with that of Dotarem. Table S1 in the Supporting Information summarizes the proton relaxivity  $r_1$  and  $r_2$  for **1a**, Dotarem, and Omniscan. The  $r_1$  and  $r_2$  of **1a** are the highest to exhibit  $6.17 \pm 0.13$  and  $6.37 \pm 0.05 \text{ mM}^{-1} \text{ s}^{-1}$  at 298 K and 128 MHz, respectively. It is worth noting that the  $r_1$  value of **1a** is twice as high as that Dotarem. A slower tumbling motion in **1a**

as a result of an increase in molecular weight achieved through conjugation with RGD may partially explain such increases in relaxivities as compared with Dotarem and Omniscan.<sup>16</sup> Moreover the radioactivity did not have any effect on magnetic relaxation. Taken together, if measured at the same concentration, three complexes (**1a**, **1b**, and **1a/1b**) are expected to show the same relaxation behavior.

Figure 3 shows in vivo dual SPECT/MR images of the integrin  $\alpha_v\beta_3$  positive U87MG tumor visualized with a mixture

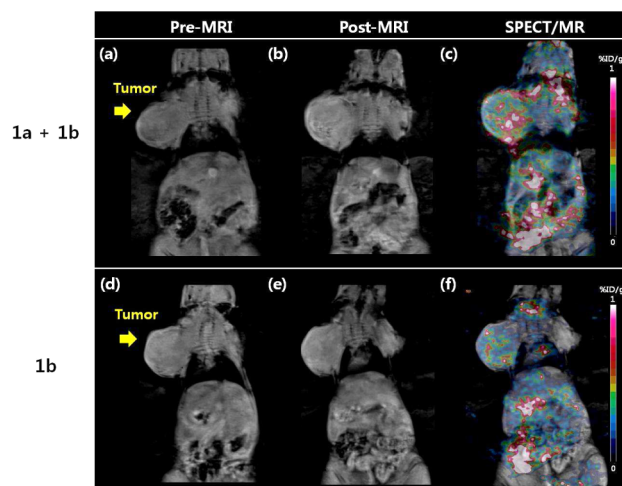


**Figure 3.** In vivo MR and SPECT/MR images of U87MG tumor-bearing mice obtained with a mixture of **1a** and **1b** (a–c) and **1b** (d–f). Quantitative analyses of SPECT imaging of tumors were  $0.56 \pm 0.05$  and  $0.24 \pm 0.09$  at c and f, respectively.

of **1a** and **1b**. To overcome the sensitivity difference, the relative amounts of **1a** and **1b** were adjusted as follows: [**1a**] for MRI = 2.7 mg (0.1 mmol Gd/kg); [**1b**] for SPECT =  $1.5 \times 10^{-5}$  mg (200  $\mu$ Ci). It is worth noting that the U87MG tumor is more clearly visualized with high contrast in SPECT by a mixture of **1a** and **1b**. Similar observations were also made with MRI as well: that is, a strong signal enhancement with a mixture of **1a** and **1b**, while it remains minimal with **1b** alone.

Figure 4 shows the tissue distribution profiles of **1b** in nude mice bearing the U87MG glioblastoma tumors. The weighted size of the dissected tumors ranges from 5 to 7 mm. Rapid clearance of radioactivity from the blood circulation is observed. Among the organs evaluated, stomach and kidney show the highest uptake (stomach,  $3.69 \pm 0.29\%$  ID/g; kidney,  $2.79 \pm$

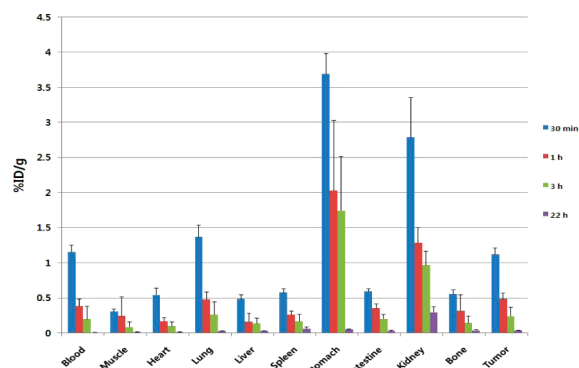


**Figure 4.** Organ uptake (% ID/g) of (**1b**) by mice ( $n = 4$ ) in 30 min and 1, 3, and 24 h.

$0.59\%$  ID/g) 30 min after injection. The high uptake by stomach may suggest partial deiodination of  $^{125}\text{I}$ . Sodium iodide symporter (NIS), which is an integral membrane protein, is known to transport two sodium ions and one iodide ion into cells in thyroid tissue, salivary glands, stomach, and breast.<sup>17,18</sup> Therefore, specific uptake by stomach, a NIS-expressing organ, suggests the possible decomposition of the  $^{125}\text{I}$ -labeled complex into iodine ion and ligand. That is, iodide is dissociated from **1b** to be taken up by stomach. The tumor also shows high uptake of **1b** ( $1.12 \pm 0.09\%$  ID/g). Here again, the behavioral difference between **1b** and a mixture of **1a/1b** can be recognized. For instance, for the reason unknown, the biodistribution profiles with a mixture of **1a/1b** exhibit radioactivity twice as high as that exhibited by **1b** alone (Figure S2 in the Supporting Information).

The molecular specific tumor imaging can be further validated by MRI imaging and MRI blocking experiments. Although MR images are acquired 90 min after administration of a mixture of **1a** and **1b**, the integrin  $\alpha_v\beta_3$  positive tumor can be still enhanced by MR because the signal for **1a** remains almost steady for 3 h (Figure 5). The CNR profile of a mixture

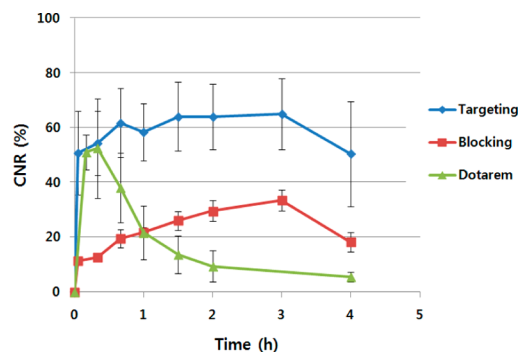


**Figure 5.** Contrast-to-noise ratio (CNR) as a function of time measured from the targeting, blocking, and Dotarem experiments by MRI.

of **1a** and **1b** shows a significant increase in CNR for as long as up to 1 h after injection, and the signal persists for 3 h. In contrast, however, the CNR profile of Dotarem shows a rapid increase within 30 min followed by a sharp drop since then. Here, steady signal enhancement by a mixture of **1a** and **1b** indicates molecular specific binding to integrin  $\alpha_v\beta_3$  in the U87MG tumor. The integrin-specific nature of a mixture of **1a** and **1b** can be further confirmed by blocking experiments as shown in Figure 5.

In summary, we successfully synthesized small molecule-based dual modal MR/SPECT imaging agents **1a** and **1b**. The BFCA consists of DOTA conjugate of cyclic RGD, where RGD incorporates a  $^{125}\text{I}/^{127}\text{I}$  moiety to the side chain amino group of the peptide to truly accomplish the chemical equivalence in the cocktail mixture of **1a** and **1b**.

## ■ ASSOCIATED CONTENT

### 📄 Supporting Information

Synthesis of **1a** and **1b** and other detailed procedures: in vitro serum stability assay, in vitro cell toxicity, relaxivity measurements, biodistribution, and in vivo imaging studies. This material is available free of charge via the Internet at <http://pubs.acs.org>.

## ■ AUTHOR INFORMATION

## Corresponding Author

\*Tel: +82-53-420-5471. Fax: +82-53-422-2677. E-mail: ychang@knu.ac.kr. (Y.C.). Tel: +82-2-970-1387. Fax: +82-2-970-2416. E-mail: kmkim@kirams.re.kr (K.M.K.).

## Funding

This work was partially supported through The Programs of Development Research Center of PET Application Technology & The Programs of Clinical Application Research of Radiopharmaceuticals in the National Nuclear Technology Program, ROK. The work was also partially supported by Nuclear R&D Program (Grant Nos. 2009-0081817 to Y.C. and 2012013722 to K.M.K.) through the National Research Foundation of Korea (NRF) funded by MEST, ROK. Kyungpook National University is also acknowledged for partial support of financial support through KNU Research Fund, 2012.

## Notes

The authors declare no competing financial interest.

## ■ REFERENCES

- (1) Jennings, L. E.; Long, N. J. 'Two is better than one'—Probes for dual-modality molecular imaging. *Chem. Commun.* **2009**, *24*, 3511–3524.
- (2) Louie, A. Multimodality Imaging Probes: Design and Challenges. *Chem. Rev.* **2010**, *110*, 3146–3195.
- (3) Khalil, M. M.; Tremoleda, J. L.; Bayomy, T. B.; Gsell, W. Molecular SPECT Imaging: An Overview. *Int. J. Mol. Imaging* **2011**, *796025*.
- (4) Pimolott, S. L.; Sutherland, A. Molecular tracers for the PET and SPECT imaging of disease. *Chem. Soc. Rev.* **2011**, *40*, 149–162.
- (5) Frullano, L.; Catana, C.; Benner, T.; Sherry, A. D.; Caravan, P. Bimodal MR-PET agent for quantitative pH imaging. *Angew. Chem., Int. Ed.* **2010**, *49*, 2382–2384.
- (6) Gianolio, E.; Maciocco, L.; Imperio, D.; Giovenzana, G. B.; Simonelli, F.; Abbas, K.; Bisi, G.; Aime, S. Dual MRI-SPECT agent for pH-mapping. *Chem. Commun.* **2011**, *47*, 1539–1541.
- (7) Cabral, H.; Nishiyama, N.; Kataoka, K. Supramolecular nanodevices: from design validation to theranostic nanomedicine. *Acc. Chem. Res.* **2011**, *44*, 999–1008.
- (8) Kwon, I. K.; Lee, S. C.; Han, B.; Park, K. Analysis on the current status of targeted drug delivery to tumors. *J. Controlled Release* **2012**, *164*, 108–114.
- (9) Mahmoudi, M.; Hofmann, H.; Rothen-Rutishauser, B.; Petri-Fink, A. Assessing the in vitro and in vivo toxicity of superparamagnetic iron oxide nanoparticles. *Chem. Rev.* **2012**, *112*, 2323–2338.
- (10) Pompa, P. P.; Vecchio, G.; Galeone, A.; Brunetti, V.; Maiorano, G.; Sabella, S.; Cingolani, R. Physical assessment of toxicology at nanoscale: Nano dose-metrics and toxicity factor. *Nanoscale* **2011**, *3*, 2889–2897.
- (11) Caravan, P.; Ellison, J. J.; McMurry, T. J.; Lauffer, R. B. Gadolinium(III) chelates as MRI contrast agents: Structure, dynamics, and applications. *Chem. Rev.* **1999**, *99*, 2293–2352.
- (12) Dirksen, A.; Langereis, S.; de Waal, B. F.; van Genderen, M. H.; Meijer, E. W.; de Lussanet, Q. G.; Hackeng, T. M. Design and synthesis of a bimodal target-specific contrast agent for angiogenesis. *Org. Lett.* **2004**, *6*, 4857–4860.
- (13) Park, J. A.; Kim, J. Y.; Kim, H. K.; Lee, W.; Lim, S. M.; Chang, Y.; Kim, T. J.; Kim, K. M. Heteronuclear Gd-<sup>99m</sup>Tc Complex of DTPA-Bis(histidylamide) Conjugate as a Bimodal MR/SPECT Imaging Probe. *ACS Med. Chem. Lett.* **2012**, *3*, 299–302.
- (14) Haubner, R.; Grätias, R.; Diefenbach, B.; Goodman, S. L.; Jonczyk, A.; Kessler, H. Structural and functional aspects of RGD-containing cyclic pentapeptides as highly potent and selective integrin  $\alpha_v\beta_3$  antagonists. *J. Am. Chem. Soc.* **1996**, *118*, 7461–7472.
- (15) Mindt, T. L.; Muller, C.; Melis, M.; de Jong, M.; Schibil, R. "Click-to-chelate": In vitro and in vivo comparison of a <sup>99m</sup>Tc(CO)<sub>3</sub>-labeled N( $\tau$ )-histidine folate derivative with its isostructural, clicked 1,2,3-triazole analogue. *Bioconjugate Chem.* **2008**, *19*, 1689–1695.
- (16) Park, J. A.; Lee, J. J.; Jung, J.-C.; Yu, D.-Y.; Oh, C.; Ha, S.; Kim, T.-J.; Chang, Y. Gd-DOTA conjugate of RGD as a potential tumor-targeting MRI contrast agent. *ChemBioChem* **2008**, *9*, 2811–2813.
- (17) Chung, J. K. Sodium iodide symporter: its role in nuclear medicine. *J. Nucl. Med.* **2002**, *43*, 1188–1200.
- (18) Kang, J. H.; Chung, J. K.; Lee, Y. J.; Shin, J. H.; Jeong, J. M.; Lee, D. S.; Lee, M. C. Establishment of a human hepatocellular carcinoma cell line highly expressing sodium iodide symporter for radionuclide gene therapy. *J. Nucl. Med.* **2004**, *45*, 1571–1576.